HHS Public Access

Author manuscript

Neurobiol Dis. Author manuscript; available in PMC 2016 October 01.

Published in final edited form as:

Neurobiol Dis. 2015 October ; 82: 164–175. doi:10.1016/j.nbd.2015.05.016.

The Developmental Evolution of the Seizure Phenotype and Cortical Inhibition in Mouse Models of Juvenile Myoclonic Epilepsy

Fazal Arain[1,2], **Chengwen Zhou**[1], **Li Ding**[1], **Sahar Zaidi**[1], and **Martin J. Gallagher**[1,*]

[1]Department of Neurology, Vanderbilt University, Nashville, TN 37232-8552 USA

Abstract

The $GABA_A$ receptor ($GABA_AR$) α1 subunit mutation, A322D, causes autosomal dominant juvenile myoclonic epilepsy (JME). Previous *in vitro* studies demonstrated that A322D elicits α1(A322D) protein degradation and that the residual mutant protein causes a dominant-negative effect on wild type $GABA_ARs$. Here, we determined the effects of heterozygous A322D knockin ($Het_{α1}AD$) and deletion ($Het_{α1}KO$) on seizures, $GABA_AR$ expression, and motor cortex (M1) miniature inhibitory postsynaptic currents (mIPSCs) at two developmental time-points, P35 and P120. Both $Het_{α1}AD$ and $Het_{α1}KO$ mice experience absence seizures at P35 that persist at P120, but have substantially more frequent spontaneous and evoked polyspike wave discharges and myoclonic seizures at P120. Both mutant mice have increased total and synaptic α3 subunit expression at both time-points and decreased α1 subunit expression at P35, but not P120. There are proportional reductions in α3, β2, and γ2 subunit expression between P35 and P120 in wild type and mutant mice. In M1, mutants have decreased mIPSC peak amplitudes and prolonged decay constants compared with wild type, and the $Het_{α1}AD$ mice have reduced mIPSC frequency and smaller amplitudes than $Het_{α1}KO$ mice. Wild type and mutants exhibit proportional increases in mIPSC amplitudes between P35 and P120. We conclude that $Het_{α1}KO$ and $Het_{α1}AD$ mice model the JME subsyndrome, childhood absence epilepsy persisting and evolving into JME. Both mutants alter $GABA_AR$ composition and motor cortex physiology in a manner expected to increase neuronal synchrony and excitability to produce seizures. However, developmental changes in M1 $GABA_ARs$ do not explain the worsened phenotype at P120 in mutant mice.

Keywords

electroencephalography; patch-clamp; Western blot; immunofluorescence; confocal microscopy; electrophysiology; brain

*To whom correspondence should be addressed: Department of Neurology, Vanderbilt University, 6114 Medical Research Building III, 465 21st Ave, South, Nashville, TN 37232-8552. Martin.Gallagher@Vanderbilt.edu; Fax: 615-322-5517; Tel.: 615-322-5979.

[2]Current Address: Department of Biological and Biomedical Sciences, The Aga Khan University, Stadium Road, P.O. Box 3500, Karachi, Pakistan.

INTRODUCTION

Juvenile myoclonic epilepsy (JME) is a common generalized epilepsy syndrome that accounts for 5-10% of all cases of epilepsy (Camfield et al., 2013). All JME patients experience myoclonic seizures, sudden, very brief jerks of a muscle or groups of muscles. (Genton et al., 2013). In addition, most JME patients experience generalized tonic-clonic (GTC) seizures, and approximately 30% of JME patients exhibit absence seizures, brief episodes of staring and loss-of-awareness (Genton et al., 2013). On electroencephalography (EEG), myoclonic seizures are typically characterized as fast (4-6 Hz), polyspike-and-wave discharges (PSD), and absence seizures are associated with very rhythmic, 3 Hz spike-wave discharges (SWD). Different JME subsyndromes can be distinguished depending on the age of onset, rates of medical intractability, as well as the presence or absence of different seizure types (Martinez-Juarez et al., 2006).

JME is classified as a genetic generalized epilepsy syndrome and it is thought to be transmitted primarily by complex genetics. However, several genes have been identified that are associated with monogenic forms of JME (Delgado-Escueta et al., 2013). Although these monogenic forms of JME are much less prevalent than the polygenic forms, they serve as invaluable models that will help elucidate the pathophysiology of the more common forms of polygenic JME.

A highly penetrant form of monogenic JME arises from a heterozygous missense mutation of the $GABA_A$ receptor ($GABA_AR$) α1 subunit (Cossette et al., 2002). $GABA_ARs$ are the main inhibitory ligand-gated ion channels in mammalian brain (Benarroch, 2007). They are pentamers composed of five subunits that arise from eight gene families; many of the gene families contain multiple isoforms (α1-6, β1-3, γ1-3, δ, ε, θ, π, ρ1-3). *In vitro* studies demonstrated that the A322D mutation causes α1(A322D) protein misfolding with altered transmembrane topology (Gallagher et al., 2007) and rapid elimination by endoplasmic reticulum associated degradation (Bradley et al., 2008;Gallagher et al., 2007). This causes a 92% reduction of total α1(A322D) subunit expression (Ding et al., 2010). In addition, when expressed *in vitro*, the residual α1(A322D) subunit protein causes a small, but significant reduction of wild type $GABA_AR$ expression. These *in vitro* data suggested that the GABRA1(A322D) mutation produces epilepsy by causing a heterozygous loss of α1 subunit and also, possibly, by a dominant-negative effect on wild type $GABA_AR$ expression.

Previously, we reported that at postnatal day 35 (P35), heterozygous Gabra1 deletion ($Het_{α1}KO$) caused SWDs and absence seizures (Arain et al., 2012) and altered $GABA_AR$ expression and physiology in the cortex and thalamus (Zhou et al., 2013;Zhou et al., 2015). These data demonstrate that heterozygous loss of α1 subunit was sufficient to cause an epilepsy phenotype. However, we did not observe any PSDs, myoclonic seizures, or GTC seizures in the P35 $Het_{α1}KO$ mice and thus they did not fully recapitulate a JME phenotype. This finding could suggest that the dominant negative effect from the α1(A322D) subunit and/or further brain development beyond P35 could be important for the production of these additional types of seizures. Therefore, we generated heterozygous Gabra1(A322D) knockin ($Het_{α1}AD$) mice and directly compared their seizure phenotypes and $GABA_A$ receptor

expression and function with those of $Het_{\alpha1}KO$ and wild type mice at two different times of development, P35 and P120.

MATERIALS AND METHODS

Animals and genotyping

All animal procedures were performed in accordance with protocols approved by the Vanderbilt University Institutional Animal Care and Use Committee (IACUC). Mice were housed in a temperature and humidity controlled environment, with a 12 hour light/dark schedule. Water and food was provided ad libitum. The $Het_{\alpha1}KO$ mice in the congenic C57BL/6J strain were described previously (Arain et al., 2012). We collaborated with the Gene Targeting and Transgenic Facility at The University of Connecticut Health Center to design the $Het_{\alpha1}AD$ knockin mice (Fig 1A). Briefly, a bacterial artificial chromosome (BAC) construct containing exon 9 of the Gabra1 subunit was modified by mutating the GCC codon with GAC to encode the A322D missense mutation. The selection cassettes, PGKneo (surrounded by loxP sequences), and MC1-HSV-TK sequence were also inserted into the BAC vector. The BAC construct was transfected into embryonic stem cells (ESC). Correct homologous recombination was confirmed using selection with G148 and ganciclovir and further verification was done using PCR and DNA sequencing. The correctly-targeted ESC were injected into growing blastocysts and implanted into pseudo-pregnant females. The offspring exhibiting chimerism were used to test for germ line transmission. These $Het_{\alpha1}AD$ mice were then crossed with mice expressing Cre driven by the hypoxanthine-guanine phosphoribosyltransferase promoter to remove the loxP flanked PGKneo cassette. The resulting $Het_{\alpha1}AD$ mouse line was verified using PCR and DNA sequencing. We used speed congenic testing (DartMouse speed congenic facility at The Geisel School of Medicine) to rapidly backcross the $Het_{\alpha1}AD$ mice into a C57BL/6J congenic line.

To directly compare the effects of heterozygous deletion and A322D knockin on epilepsy phenotypes and on $GABA_AR$ expression and function and to control for environmental effects, we used mice that had wild type, $Het_{\alpha1}KO$, and $Het_{\alpha1}AD$ mice within the same litter. Therefore, we mated $Het_{\alpha1}KO$ and $Het_{\alpha1}AD$ mice to produce wild type, $Het_{\alpha1}KO$ and $Het_{\alpha1}AD$ mice in a 1:1:1 ratio; as expected, the compound heterozygous $Het_{\alpha1}KO/Het_{\alpha1}AD$ mice died at approximately P15-P19 similar to the homozygous Gabra1 deletion mice ($Hom_{\alpha1}KO$) we reported previously (Arain et al., 2012). We also bred $Het_{\alpha1}AD$ mice to produce homozygous Gabra1(A322D) mice ($Hom_{\alpha1}AD$) that were used to determine the effects of the A322D mutation on α1(A322D) subunit protein expression; as a control, these experiments also included protein from $Hom_{\alpha1}KO$ which were bred from $Het_{\alpha1}KO$ parents.

In initial experiments, we verified that the correct codon was mutated by sequencing tail genomic DNA. We amplified the genomic DNA using the 5'-GGAGAGTACTCTATCTCTTCTG-3' and 5'-GGTTATCTGTGTGGCTCACG-3' primers, purified the amplified DNA on an agarose gel, and performed Sanger sequencing on the purified DNA with the same primers that were used for amplification. After we verified that the mutation was introduced correctly, we genotyped mice for all subsequent experiments using tail DNA with forward primer, 5'-CGTGAGCCACACAAATAACC-3' and the

reverse primer, 5'-ACCCTTTGATGGGTTACAGC-3'. Genotyping wild type and $Het_{\alpha 1}AD$ DNA produced DNA bands of 324 bp and 407 bp, respectively. Genotyping the $Het_{\alpha 1}KO$ mice was performed as described previously (Arain et al., 2012).

With this breeding strategy, we did not find any sex-dependent effect on epileptiform discharges or seizures and thus grouped males and females together for the EEG experiments. However we used females for the Western blots, immunofluorescence studies, and electrophysiology experiments in order to enable comparison with the prior studies (Zhou et al., 2015;Zhou et al., 2013). We tested the mice in two age groups P33-38 (identified as "P35" in the text) and P120-P130 (identified as "P120" in the text).

Video/EEG monitoring of spontaneous and evoked epileptiform discharges

As described previously (Arain et al., 2012), we surgically implanted prefabricated mouse EEG headmounts that record two bipolar EEG channels and one subcutaneous nuchal EMG channel (Pinnacle Technologies). The surgeries were performed at least 48 hours prior to the EEG. For the initial experiments, we recorded EEG at P35 and P45 and at every subsequent 15 ± 3 days until P120. These preliminary longitudinal experiments determined that the incidence of spontaneous PSDs and myoclonic seizures was substantially more frequent at P120 than earlier ages. Therefore, for subsequent experiments, we recorded video/EEG from mice implanted at approximately P35 or P120.

The EEG and video data were analyzed by a blinded reviewer to identify SWDs, PSDs and myoclonic seizures. SWDs were identified using criteria described previously and consisted of highly rhythmic 6-8 Hz waveforms (Arain et al., 2012;Akman et al., 2010;Sitnikova & van Luijtelaar, 2007). PSDs were identified as described previously (Garcia-Cabrero et al., 2012) and consisted of very brief (< 0.5 second), high frequency (approximately 50 ms interspike interval) complexes with voltages at least twice the background voltage. The two morphological features that differentiated SWDs and PSDs were that SWDs had a lower spike frequency (interspike interval 125-166 Hz), and a much higher rhythmicity than the PSDs. To quantify the differences in initial spike frequency between SWDs and PSDs, we also used the EDFbrowser software (Teunis van Beelen) to calculate the spectral density (5-30 Hz in 5 Hz bins) of the first 200 ms in a systematic sample of PSDs and SWDs from P120 $Het_{\alpha 1}KO$ and $Het_{\alpha 1}AD$ mice and compared the combined high frequency (15-30 Hz) spectral density between SWDs and PSDs.

Myoclonic seizures were identified on video. Ten second video/EEG segments encompassing PSD complexes was manually reviewed and we compared the incidence of visible myoclonic seizures occurring during the PSD and during the other ten seconds of recording without a PSD. The probability of a myoclonic seizure during the PSD complex was compared to a myoclonic-like movement during the other ten seconds of video.

In addition to determining the effects of genotype and age on spontaneous SWDs and PSDs, we also determined their effects on pentylenetetrazol- (PTZ) evoked PSDs / myoclonic seizures and GTC seizures. We adapted the procedure published by Wong et al that used repeated, low-dose intraperitoneal PTZ to provoke PSD and myoclonic seizures and, sometimes, GTC seizures (Wong et al., 2003). Briefly, mice were first injected with 25

mg/kg PTZ and then, 45 minutes later, four “booster” doses of 10 mg/kg PTZ were administered intraperitoneally ten minutes apart. If a GTC seizure occurred during the course of the experiment, no further doses of PTZ were given. We recorded the mean PSD frequency during the course of the experiment as well as the latency of each PSD relative to the first PTZ injection (time 0). In addition, we determined whether or not a PTZ-induced GTC seizure occurred and the GTC seizure latency.

Antibodies

For Western blots and immunohistochemistry experiments, we used the antibodies with the dilutions listed in Table 1.

Western blots

Western blot experiments were conducted as described previously (Zhou et al., 2013). Briefly, mice were anesthetized with isoflurane and euthanized and their brains were removed from the skull. For the initial experiments that determined the effects of $Hom_{\alpha1}KO$ and $Hom_{\alpha1}AD$ on α1 and α1(A322D) subunit protein, we utilized young mice (P15-P18) because the homozygous mice experienced a very high mortality at later ages; these experiments analyzed protein obtained from the entire cortex. For the experiments that determined the effects of $Het_{\alpha1}KO$ and $Het_{\alpha1}AD$ on $GABA_AR$ subunit expression, we used P35 and P120 mice and generated 2 mm coronal block slices that contained the sensorimotor cortex before dissecting the cortex from the subcortical tissue. The cortical sections were sonicated in radioimmunoprecipitation assay (RIPA) solution (20 mm Tris, pH 7.4, 1% Triton X-100, 250 mm NaCl, 0.5% deoxycholate, and 0.1% SDS) that also contained protease inhibitor mixture (1:100; Sigma-Aldrich). Protein concentrations were determined using a copper/bicinchoninic acid-based assay (Thermo Scientific). Proteins were fractionated on 10% SDS-polyacrylamide gels and then electrotransferred to nitrocellulose membranes. The blots were stained with fluorescently-conjugated secondary antibodies which were visualized using an infrared imaging system (LiCor). To ensure linearity of detection, at least two masses of each protein lysate were analyzed on the gels and we confirmed that the changes in protein intensity corresponded to the mass of lysate loaded on the gel. We were able to directly compare the relative expression of $GABA_AR$ subunit proteins among the three genotypes at P35 and P120 by loading samples from all three genotypes from both ages on the same gel. We measured the background-subtracted protein band intensity multiplied by the band area (integrated intensity) of each detected $GABA_AR$ subunit and divided that value by the integrated intensity of actin (loading control).

Immunofluorescence

Immunofluorescence experiments were performed as previously described (Zhou et al., 2015). Mice were euthanized as described above and 2 mm block slices containing the sensorimotor cortex were generated. The block slices were briefly fixed in paraformaldehyde using the protocol of Schneider Gasser et al. in order to best visualize the synaptic protein clusters (Schneider Gasser et al., 2007). After fixation and cryoprotection, 15 μm coronal slices were generated on a cryostat (Lyca). As described previously (Zhou et al., 2015), the slides were incubated with primary and secondary antibodies (Table 1) and mounted using a solution that also contained 4',6-diamidino-2-phenylindole (DAPI) to stain

cell nuclei. Images were acquired using an Olympus FV-1000 confocal microscope using a 100X, 1.40 NA SPlan-UApo oil immersion lens using settings to obtain a slice 1 μm thick and with a resolution of 82 nm/pixel. All images were obtained from cortical layers II/III and V/VI in the primary motor cortex and primary somatosensory cortex as well as in the subcortical white matter. Cortical layers were identified based on their distance from the pia and subcortical white matter as well as the pattern of DAPI staining.

The immunofluorescence images were analyzed using Image J software (National Institutes of Health). This short fixation protocol (Schneider Gasser et al., 2007) maximizes the identification of clustered synaptic proteins, but often results in slice to slice differences in absolute fluorescence. Therefore, we quantified differences in the relative distribution of $GABA_AR$ subunits within the same slice and not fluorescence values among different slices. The background values were defined as the mean fluorescence in the subcortical white matter and diffuse staining was defined as the average fluorescence intensity of four regions within an image that did not include any α1 or α3 subunit or gephyrin clusters. Total staining was defined as average staining of the whole image minus the background staining. Gephyrin clusters were identified automatically as regions (0.1-2 μm^2) in which the gephyrin staining intensity was at least three-fold higher than the diffuse staining

We first determined if the mutations changed the relative distribution of total α1 or α3 subunit staining between the upper (II/III) and lower (V/VI) layers of the somatosensory and motor cortices at either the P35 or P120 time-points. We next determined the effects of the mutations and age on gephyrin cluster density and size. Finally, we calculated the α1 and α3 subunit synaptic cluster ratio (SCR) as the amount of background-subtracted α1 and α3 subunit staining intensity at each gephyrin cluster relative to the total α1 and α3 subunit staining (Zhou et al., 2015).

Electrophysiology

Brain slice patch clamp electrophysiology studies were performed as described previously (Zhou et al., 2015). The external solution was (in mM) 126 NaCl, 2.5 KCl, 1.25 NaH_2PO_4, 2 $CaCl_2$, 1 $MgCl_2$, and 10 D-glucose, pH 7.4. Tetrodotoxin (1 μM) and 2,3-dihydroxy-6-nitro-7-sulfamoyl-benzo[f]quinoxaline-2,3-dione (NBQX, 20 μM) were added to block sodium channels and AMPA receptors. The internal solution contained 135 CsCl, 10 EGTA, 10 HEPES, 5 ATP-Mg, and 5 QX-314 (pH 7.3, 290-295 mOsm). The filled patch pipettes had resistances of 2 - 4 MΩ. We identified pyramidal neurons in layer II/III of motor cortex and performed patch clamp studies at room temperature and with a holding potential of −60 mV using a MultiClamp 700B amplifier (Molecular Devices Inc.) and Clampex 10.2 software (Molecular Devices Inc.). Serial resistance was monitored continuously and recordings were discarded if the serial resistance changed by more than 20% or 25 MΩ. The mIPSCs were automatically identified offline with the Clampfit 10.2 software and the peak amplitude, frequency, 10-90% rise time, and charge transfer were calculated. We also fit the decay phase of the mIPSCs to a single exponential function and calculated the decay constant, τ. For each cell, the median peak amplitude, rise time, decay τ and charge transfer were determined. For statistics, we compared the average of the median amplitude, rise time, decay τ and frequency obtained from the different cells. Because the median charge transfer

values from the different cells were not normally distributed, we compared rank-transformed median charge transfer values as described below.

Statistical Analyses

The three-way contingency analysis for PTZ-evoked GTCs was performed using the VassarStats Website for Statistical Computation (Vassar College). All other statistical analyses were performed using the R 3.1.1 Statistical Package for Windows (R Foundation for Statistical Computing) that also contained the lme4 and multicomp packages. Normally distributed data (seizure incidence, relative Western blot intensity, gephyrin cluster size and area, mIPSC amplitude, frequency, rise time and decay τ) are presented as the mean ± standard error of the mean (SEM). Except for Western blot intensity, these normally distributed data were compared with a two factor ANOVA test. We first used the two factor ANOVA to test for significant interactions between age and genotype. If there was no significant interaction between these two factors, we treated them as independent factors and depicted the effects of genotype and age separately in the figures. After the two factor ANOVA, statistical significance of the differences among the groups was evaluated with the Tukey honest significant difference test. We used a repeated measure t-test with Bonferroni correction to test the differences among P15 wild type, $Het_{\alpha 1}AD$ and $Hom_{\alpha 1}AD$ protein. To approximate a repeated-measure, two factor ANOVA for the Western blot data from the P35 and P120 wild type and mutant mice, we created mixed effect linear models that related integrated band intensity to the fixed factors, age and genotype, and the random effect that accounted for gel-to-gel variability between the intensity of the $GABA_AR$ subunit of interest and the loading control, actin. We made models that successively added each factor and then compared the statistical significance among the model fits using an ANOVA test. Once the best-fitting model was found, we determined the significant difference among the means of fixed factors using the general linear hypothesis test and the means were adjusted using Tukey's method.

Non-normally distributed data (SCR, charge transfer area) are shown on a box plot and are listed in tables as the median along with the first and third quartile values. We determined the significant differences among these values by rank-transforming the data and then performing the two factor ANOVA as described above. We used a three way contingency test and χ^2 test to determine the effects of age and genotype on the probability of PTZ-evoked GTCs. The significance of the differences in the distribution of PTZ-evoked PSDs was determined using the Kolmogorov-Smirnov test.

RESULTS

Initial characterization of the $Het_{\alpha 1}AD$ and $Hom_{\alpha 1}AD$ mice

The GCC → GAC point mutation was introduced into Gabra1 exon 9 to generate $Het_{\alpha 1}AD$ mice (Fig 1A). Correct targeting was confirmed by DNA sequencing (not shown) and genotyping was performed by PCR (Fig 1B). Previous studies determined the effect of the A322D mutation on α1(A322D) subunit protein expression by overexpressing α1(A322D) subunit cDNA in heterologous cells. Bradley et al. expressed epitope-tagged FLAG-α1(A322D) subunit protein along with the β2 subunit and found that the A322D mutation

reduced FLAG-α1(A322D) subunit protein expression to 44% of control (Bradley et al., 2008) whereas we previously reported that, when expressed with β2 and γ2 subunits, the untagged α1(A322D) subunit protein was reduced to 8% of control (Ding et al., 2010). To determine the effect of the A322D mutation on α1(A322D) subunit protein expression in $Hom_{α1}AD$ mice, we bred $Het_{α1}AD$ mice to produce wild type, $Het_{α1}AD$, and $Hom_{α1}AD$ pups and measured the relative amounts of cortical α1 and α1(A322D) subunit protein by Western blot. We performed the Western blots at age P15 because the $Hom_{α1}AD$ pups experienced substantial mortality beginning at P19 (not shown), a similar finding to that we observed in $Hom_{α1}KO$ mice in the C57BL6/J strain (Arain et al., 2012). The Western blots demonstrated that, at P15, $Het_{α1}AD$ and $Hom_{α1}AD$ mice express 52 ± 7% and 6 ± 3%, respectively, the amount of α1 subunit protein as wild type mice (Fig 1C). This reduction in α1 subunit expression is similar to what we observed with recombinant expression in heterologous cell culture (8%, Ding et al., 2010). For comparison, $Hom_{α1}KO$ mice did not express any detectable α1 subunit expression (not shown).

Both $Het_{α1}KO$ and $Het_{α1}AD$ mice have SWDs and absence seizures at P35 that persist at P120

To directly test the effects of $Het_{α1}KO$ and $Het_{α1}AD$ on seizure phenotype without the potentially confounding effects of the mice being raised in different litters, we mated $Het_{α1}KO$ with $Het_{α1}AD$ mice to produce wild type, $Het_{α1}KO$ and $Het_{α1}AD$ pups. The compound heterozygous $Het_{α1}KO/Het_{α1}AD$ pups, like $Hom_{α1}KO$ (Arain et al., 2012) and $Hom_{α1}AD$ pups, died shortly after P19, and thus were not studied.

Because preliminary longitudinal experiments suggested a difference in PSD frequency between P35 and P120, we performed synchronized video/ EEG recordings in wild type, $Het_{α1}KO$ and $Het_{α1}AD$ mice at these two time-points. Both $Het_{α1}KO$ and $Het_{α1}AD$ mice exhibited abundant SWDs and absence-like seizures at P35 and P120 (Fig 2, Table 2). The morphology of the SWDs in both genotypes at both time-points matched those we reported previously in P35 $Het_{α1}KO$ (Arain et al., 2012) and those that have been reported for rat SWD and AS (Akman et al., 2010;Robinson & Gilmore, 1980;Sitnikova & van Luijtelaar, 2007). Specifically, each SWD consisted of very rhythmic, 6-8 Hz spikes, positive transients, and waves (Fig 2C-D). Synchronized video recordings demonstrated that these SWDs were associated with behavioral arrest indicating that they were behavioral, as well as electrographic absence-like seizures (not shown).

As reported previously (Arain et al., 2012;Reid et al., 2011), wild type mice exhibit a low baseline incidence of spontaneous SWDs (1.1 ± 0.3 SWD/hr, Fig 2E). However, $Het_{α1}KO$ and $Het_{α1}AD$ mice had significantly higher incidences of SWDs than wild type mice ($Het_{α1}KO$ 10.5 ± 2.4 SWD/hr, $P = 0.011$ vs wild type; $Het_{α1}AD$ 15.8 ± 2.6 SWD/hr, $P < 0.001$ vs wild type, Fig 2E). There was no significant difference in the incidence of SWDs between $Het_{α1}KO$ and $Het_{α1}AD$ mice ($P = 0.189$, Fig 2E). There was also no significant difference between the incidence of SWDs between P35 and P120 mice ($P = 0.628$, Fig 2E), and no significant interaction between age and genotype ($P = 0.857$).

Spontaneous PSDs are more frequent in mutant mice and at P120 than P35

Continuous video/EEG revealed that P120 $Het_{\alpha1}KO$ and $Het_{\alpha1}AD$ mice exhibited a different type of discharge than SWDs. In contrast to SWDs, which are characterized by very regular spikes and waves occurring with an interspike interval of 125-166 ms, this different waveform started with two or more consecutive spikes and / or waves and occurred with an irregular periodicity and a high frequency (interspike interval 50-100 ms, Fig 3A-D). The high frequency of the waveforms during the first 200 ms of the discharges resulted in a significantly increased spectral density in the high frequency range (15-30 Hz) relative to SWDs (Fig 3G, $P < 0.001$). There was no difference in high frequency spectral density between $Het_{\alpha1}KO$ and $Het_{\alpha1}AD$ mice ($P = 0.574$). In addition to having a different rhythmicity and frequency, these discharges also had a substantially shorter duration (0.35 ± 0.02 s) than SWDs (2.0 ± 0.4 s). Because the features of these complexes resembled the polyspike discharges reported previously in a mouse model of Lafora-type progressive myoclonic epilepsy (Garcia-Cabrero et al., 2012) we designated them PSDs.

Consistent with human JME, only a portion of PSDs in the mice were associated with visible myoclonus. Analysis of the synchronized video revealed that 15% of PSDs from $Het_{\alpha1}KO$ mice and 10% of the PSDs from $Het_{\alpha1}AD$ mice were associated with visible myoclonic jerks (Supplementary video 1). Sampling the video at times when PSDs were not present revealed that these behavioral jerks were not present in the absence of the electrographic PSDs.

These spontaneous PSDs and myoclonic seizures were very infrequent compared with the SWDs. Quantification of the PSDs showed that both genotype and age significantly affected the PSD incidence (Fig 3E). $Het_{\alpha1}KO$ mice exhibited 2.1 ± 0.6 PSDs/day ($P = 0.020$ vs. wild type), $Het_{\alpha1}AD$ mice had 1.9 ± 0.5 PSD/day ($P = 0.016$ vs. wild type) and wild type mice had 0.3 ± 0.2 PSDs/day. In addition, there were significantly more PSDs at P120 (2.4 ± 0.5 PSDs/day) than P35 (0.6 ± 0.2, $P = 0.001$). There was no significant interaction between genotype and age ($P = 0.362$) and no significant difference in the PSD incidence between $Het_{\alpha1}KO$ and $Het_{\alpha1}AD$ mice ($P = 0.980$). Additionally, there was no substantial linear correlation ($r^2 \leq 0.24$) between the SWD and PSD incidence within individual mice (Fig 3F), a result that suggests PSDs and SWDs are truly distinct events and that PSDs did not simply represent SWD fragments.

Although the majority of JME patients experience GTC seizures as well as myoclonic seizures, the GTC seizures occur substantially less frequently (one-two per year) than myoclonic seizures (several each day, Genton et al., 2013). Consistent with the low frequency of GTC seizures found in human patients, we recorded one spontaneous GTC seizure in a P120 $Het_{\alpha1}KO$ mouse and one in a P120 $Het_{\alpha1}AD$ mouse (not shown). There were no spontaneous GTC seizures recorded in wild type or P35 mice.

Effects of Gabra1 disruption and development on PTZ-evoked seizures

We next determined the effect of $Het_{\alpha1}KO$ and $Het_{\alpha1}AD$ on PTZ-evoked seizures at P35 and P120 (Fig 4, Table 2). The morphology of the PTZ-evoked PSDs (Fig 4A-D) was similar to the spontaneous PSDs (Fig 3). Consistent with spontaneous PSDs, there was a

substantial effect of age on PSD frequency with increased PTZ-evoked PSDs in P120 mice (6.3 ± 1.8 PSD/hr) compared with P35 mice (0.7 ± 0.3 PSD/hr, P = 0.006, Fig 4E). As seen previously, PTZ evoked PSDs in wild type mice as well as mutant mice; there was no significant difference in the PSD frequency among the genotypes (P ≥ 0.103, Fig 4E). However, the PSDs in P120 $Het_{\alpha 1}KO$ (median PSD latency = 49.7 minutes) and $Het_{\alpha 1}AD$ mice (median PSD latency = 47.3 minutes) occurred with a higher probability at shorter latencies after PTZ injection than in wild type mice (median PSD latency = 69.9 minutes, P < 0.001, Fig 4F).

Although we administered a low dose of PTZ, some mice did develop GTC seizures. There was no difference among the genotypes in the GTC seizure latency (not shown) or incidence (Fig 4F, P = 0.418). However, consistent with the spontaneous and evoked PSDs, there was a substantially higher incidence of evoked GTC seizures in P120 mice (58.8%) than P35 mice (6.7%, P = 0.002), a finding that suggested greater cerebral excitability at this age.

Altered cortical $GABA_AR$ expression in $Het_{\alpha 1}KO$ and $Het_{\alpha 1}AD$ mice

The subunit composition of $GABA_A$ receptors governs many of the channel properties including the agonist EC_{50}, peak synaptic current amplitude, the time course of synaptic current kinetics, and the response to pharmacological agents (Gonzalez, 2013). Therefore, we performed Western blots and immunofluorescence/confocal microscopy experiments to determine the total expression and synaptic localization of $GABA_AR$ subunits at P35 and P120 in the cortices of $Het_{\alpha 1}KO$ or $Het_{\alpha 1}AD$ mice. For this study, we chose to focus on the cortex, and not thalamic nuclei, because EEG discharges reflect cortical neuronal activity (albeit highly innervated by subcortical regions), and because human electrophysiological studies have shown that JME is associated with cortical disinhibition (Badawy et al., 2013). Moreover, cortical neurons express multiple isoforms of $GABA_AR$ α subunits (Hortnagl et al., 2013) and the amount of protein expression of these α subunits decreases between P30 and P90 (Yu et al., 2006); therefore, we hypothesized that this change in cortical α subunit expression may be related to the developmental change in seizure phenotype.

Before performing the Western blots, we verified that neither $Het_{\alpha 1}KO$ nor $Het_{\alpha 1}AD$ altered the expression of the loading control protein, actin, at either P35 or P120 (P ≥ 0.136, not shown). Therefore, we were able to compare the relative expression of the $GABA_AR$ subunits in the three genotypes and at the two ages by normalizing the integrated band density of each subunit to actin.

Western blots of frontal cortex protein demonstrated that while genotype did not affect the relative expression of β2/3 (P = 0.677, Fig 5A) or γ2 subunit protein (P = 0.585, Fig 5B), aging from P35 to P120 reduced the expression of β2/3 (75 ± 6% vs. P35, P < 0.001, Fig 5A) and γ2 subunit (74 ± 5% vs. P35, P < 0.001, Fig 5B) protein. Because the vast majority of $GABA_ARs$ contain β2/3 and/or γ2 subunits, these data suggest that total expression $GABA_AR$ (of all isoforms) is not affected by genotype, but is reduced by approximately 25% from P35 to P120 in frontal cortices.

Next, we determined the effects of heterozygous α1 subunit deletion and A322D substitution on α1 and α3 subunit expression in the frontal cortex. Age interacted with

genotype to affect α1 subunit expression (Fig 5C, age / genotype interaction $P < 0.001$). The nature of the interaction of age with genotype was surprising. At P35, as expected, α1 subunit deletion/mutation reduced total α1 subunit expression, although only the reduction in $Het_{\alpha1}AD$ mice (48 ± 8% vs. P35 wild type, $P = 0.002$), and not $Het_{\alpha1}KO$ mice (67 ± 8% vs P35 wild type, $P = 0.077$), was statistically significant. There was no significant difference in α1 subunit expression between $Het_{\alpha1}KO$ and $Het_{\alpha1}AD$ mice ($P = 0.878$). At P120, there was no difference in α1 subunit expression among the three genotypes ($P \geq 0.463$) and the α1 expression in each of the genotypes of mice was reduced relative to P35 wild type (wild type 48 ± 8%, $Het_{\alpha1}KO$ 52 ± 6%, $Het_{\alpha1}AD$ 61 ± 9% vs. P35 wild type, $P \leq 0.007$). Therefore, the finding that wild type cortices, but not $Het_{\alpha1}KO$ and $Het_{\alpha1}AD$ cortices, undergo a developmental reduction of α1 subunit expression indicates that the cortices partially compensate for heterozygous Gabra1 disruption at P120 by driving additional α1 subunit protein expression from their residual wild type allele.

Both age and genotype affected α3 subunit expression (Fig 5D), but there was not a significant interaction between these two factors. Consistent with our previous observations in P35 $Het_{\alpha1}KO$ mice (Zhou et al., 2013), both Gabra1 deletion (221 ± 25% vs. wild type, $P < 0.001$) and A322D knockin (204 ± 29% vs wild type, $P < 0.001$) increased cortical α3 subunit expression. In all three genotypes, there was a reduction in α3 subunit expression at P120 (68 ± 6%, $P = 0.002$) compared with P35. Surprisingly, relative to wild type, α3 subunit expression remained elevated in the mutant genotypes at P120 even though there was no longer any difference in α1 subunit expression.

While Western blots provide excellent semiquantitative measures of $GABA_AR$ subunit protein expression, they cannot identify changes in the distribution of the protein expression among different cortical layers. Therefore, we next used immunofluorescence to determine if age and/or genotype changed the distribution of α1 and α3 subunit between the upper (layers II/III) and lower (layers V/VI) cortical layers. Neither age, nor genotype altered the ratio of α1 subunit or α3 subunit immunofluorescence between the upper and lower layers of the motor or somatosensory cortices (not shown, $P \geq 0.224$). As seen previously (Pirker et al., 2000), expression of α3 subunit was increased in the lower layers of the motor (133 ± 7%) and somatosensory (134 ± 7%) cortex and α1 subunit expression was increased in the upper layers (motor cortex, 130 ± 9%, somatosensory, 176 ± 13%). These data suggest that the differences in $GABA_AR$ subunit protein expression found in the Western blots was not localized to specific cortical layers.

Next, we determined if Gabra1 knockout or A322D knockin altered α1 or α3 subunit association with the GABAergic postsynaptic marker, gephyrin in layer II/III of the motor cortex (M1, Fig 6-7). We focused on the M1 cortical region because neurophysiological and imaging studies have implicated M1 in human JME (Badawy et al., 2013;Bartolini et al., 2014;Vollmar et al., 2012). We stained brain slices with antibodies against gephyrin, α1 subunit, and α3 subunit. First, we found that neither genotype ($P \geq 0.340$) nor age ($P = 0.074$) significantly alters gephyrin cluster density. Although genotype did not change the mean gephyrin cluster area ($P \geq 0.367$), clusters were slightly larger at P120 (0.22 ± 0.00 μm^2) than at P35 (0.20 ± 0.01 μm^2, $P = 0.002$).

We then determined whether genotype and/or development changed the fraction of total α1 and α3 subunit staining associated with gephyrin clusters. Surprisingly, even though Gabra1 deletion and A322D substitution alter the total amount of α1 and α3 subunit protein (Fig 5C-D), the ratio of total α1 ($P \geq 0.751$, Fig 6G) and α3 ($P \geq 0.194$, Fig 7G) subunit associated with gephyrin was not changed in either $Het_{\alpha 1}KO$ or $Het_{\alpha 1}AD$ mice. However, at P120, in all genotypes, there was a smaller fraction of gephyrin-associated α1 subunit (P120 median 3.9, 1^{st}-3^{rd} quartile: 3.4-4.7; P35 median 5.2, 1^{st} – 3^{rd} quartile 4.0 – 5.6, $P = 0.060$) and α3 subunit (P120 median 3.7, 1^{st}-3^{rd} quartile: 3.1-4.3; P35 median 4.4, 1^{st} – 3^{rd} quartile 3.7 – 5.8, $P = 0.013$), although the change in α1 subunit was not statistically significant.

Gabra1 deletion and A322D substitution reduced mIPSC amplitudes and increased the timecourse of current decay at P35 and P120

Next, we determined the effects of heterozygous α1 subunit deletion and A322D substitution on synaptic $GABA_AR$ currents in layer II/III pyramidal neurons (Fig 8, Table 3). Compared with the peak mIPSC amplitude in wild type cortex (−31.9 ± 3.0 pA), mIPSC amplitudes were reduced in both $Het_{\alpha 1}KO$ cortex (−23.8 ± 2.1 pA, $P = 0.037$) and $Het_{\alpha 1}AD$ cortex (−16.3 ± 1.3 pA, $P < 0.001$, Fig 8B). Interestingly, the difference in mIPSC peak amplitudes between $Het_{\alpha 1}KO$ and $Het_{\alpha 1}AD$ cortex was statistically significant ($P = 0.034$) indicating a dominant negative effect from the missense mutation. In addition to the effects of genotype, mIPSC amplitudes increased during development from −21.0 ± 1.6 pA at P35 to −26.5 ± 2.4 pA at P120 ($P = 0.030$). There was no significant interaction between age and genotype ($P = 0.745$).

The timecourse of mIPSC kinetics were also altered in $Het_{\alpha 1}KO$ and $Het_{\alpha 1}AD$ mice (Fig 8C-D). The 10-90% rise times were increased from (1.3 ± 0.1 ms) in wild type mice to 2.0 ± 0.2 ms in $Het_{\alpha 1}KO$ mice ($P = 0.010$ vs. wild type) and 2.2 ± 0.2 ms in $Het_{\alpha 1}AD$ mice ($P < 0.001$ vs. wild type). Similarly, the timecourse of current decay (decay τ) was prolonged from 7.9 ± 0.8 ms in wild type mice to 12.6 ± 1.1 ms in $Het_{\alpha 1}KO$ mice ($P = 0.021$) and 13.1 ± 1.4 ms in $Het_{\alpha 1}AD$ mice ($P = 0.007$). There was no significant effect of age on rise time or decay τ ($P \geq 0.079$), and no significant difference between $Het_{\alpha 1}KO$ and $Het_{\alpha 1}AD$ in either of these current kinetic parameters ($P \geq 0.677$).

The reduced mIPSC amplitudes and increased decay τ in $Het_{\alpha 1}KO$ and $Het_{\alpha 1}AD$ cortices caused corresponding changes in charge transfer. The substantially reduced amplitude in $Het_{\alpha 1}AD$ mice caused it to have the lowest charge transfer (median 224 pA• ms, 1^{st}-3^{rd} quartile: 147-352 pA • ms) that was significantly lower than the charge transfer in wild type (median 441 pA• ms, 1^{st}-3^{rd} quartile: 245-496 pA • ms, $P = 0.011$) and $Het_{\alpha 1}KO$ (median 448 pA • ms: 1^{st}-3^{rd} quartile: 313-630 pA • ms, $P = 0.001$) M1 cortices. Even though mIPSCs in $Het_{\alpha 1}KO$ cortices were of reduced amplitude than those in wild type, the increased decay τ in $Het_{\alpha 1}KO$ cortices resulted in the lack of a significant difference in charge transfer between the two genotypes ($P = 0.773$). Like peak current amplitude, charge transfer also increased from P35 to P120 from a median of 264 pA • ms (1st-3rd quartile: 177-445) to 432 pA • ms (1st-3rd quartile 276-504 pA • ms, $P = 0.036$).

There was an unexpected effect of genotype on mIPSC frequency with the frequency in wild type cortex (4.5 ± 0.4 Hz) in-between that of $Het_{\alpha 1}KO$ (6.9 ± 1.1 Hz) and $Het_{\alpha 1}AD$ (3.1 ±

0.8 Hz) cortex. Although there was no significant difference in mIPSC frequency between wild type and either $Het_{\alpha1}KO$ or $Het_{\alpha1}AD$ cortex ($P \geq 0.154$), the frequency in $Het_{\alpha1}AD$ was statistically reduced compared with $Het_{\alpha1}KO$ ($P = 0.006$). Thus, A322D substitution caused a dominant negative effect on mIPSC frequency as well as peak amplitude. There was no significant effect of age on mIPSC frequency ($P = 0.178$).

DISCUSSION

Here, we determined the effects of heterozygous Gabra1 deletion and A322D substitution on seizures and cortical $GABA_AR$ expression at P35 and P120. Directly comparing $Het_{\alpha1}KO$ mice with $Het_{\alpha1}AD$ mice from the same litter allowed us to distinguish the effects of haploinsufficiency (i.e. effects resulting from the absence of one Gabra1 allele that occur in $Het_{\alpha1}KO$ mice) from dominant negative effects (effects resulting from expression of mutant and wild type gene products in the same cell that occur in $Het_{\alpha1}AD$ mice). There are three main conclusions from this study: 1) Even though there is a dominant negative effect of the A322D mutation on mIPSC amplitude and frequency, heterozygous loss of Gabra1 function, without a dominant negative effect, is sufficient to cause PSDs and myoclonic seizures, 2) $Het_{\alpha1}KO$ and $Het_{\alpha1}AD$ mice model the JME subsyndrome, CAE persisting and evolving into JME (CAE/JME), with absence seizures at P35 and myoclonic seizures that occur later in development, and 3) Gabra1 deletion and A322D substitution alter M1 cortical $GABA_AR$ expression and physiology in a manner that would be expected to cause disinhibition, hypersynchrony and seizures at both P35 and P120; other mechanisms besides altered $GABA_AR$ expression in M1 are responsible for the developmental change in seizure phenotype.

Heterozygous loss of Gabra1 is sufficient to cause myoclonic seizures

We demonstrated previously that, when overexpressed *in vitro*, α1(A322D) subunit protein produces a dominant negative effect by interacting with wild type $GABA_ARs$ and reducing their cell surface expression and altering $GABA_AR$ physiology (Ding et al., 2010). Here, we found that, *in vivo*, heterozygous expression of α1(A322D) subunit did not produce a dominant negative effect on $GABA_AR$ expression or synaptic clustering, but did produce a dominant negative effect on mIPSC peak current amplitudes and frequency. Nevertheless, the apparent dominant negative effect of α1(A322D) subunit on GABAergic physiology did not translate into a different seizure phenotype for $Het_{\alpha1}KO$ and $Het_{\alpha1}AD$ mice, at least between ages P35 to P120. Although, it is possible that the seizure phenotypes of the $Het_{\alpha1}KO$ and $Het_{\alpha1}AD$ mice could diverge at time-points after P120, it is also possible that heterozygous loss of α1 subunit function alone is sufficient to cause a myoclonic epilepsy phenotype (i.e. that heterozygous loss of α1 subunit produces a floor effect on seizure phenotype and that greater reductions in cortical synaptic $GABA_AR$ currents do not worsen the seizures). Importantly, the experiments conducted here evaluated only the effects of the mutations on seizures and not other neurobehavioral phenotypes. Possibly, the smaller synaptic $GABA_AR$ currents in $Het_{\alpha1}AD$ mice could result in other types of neurobehavioral abnormalities not evaluated here.

GABRA1 mutations have been associated with several other genetic generalized epilepsy syndromes besides JME (Carvill et al., 2014;Lachance-Touchette et al., 2011;Maljevic et al., 2006). In particular, a *de novo* DNA deletion/frameshift mutation (975delC/ S326fs328X) was found in a patient with CAE. Importantly, when this *de novo* mutation is expressed *in vitro* as a minigene, the mutant gene product was completely degraded and thus the 975delC/ S326fs328X mutation approximates a heterozygous GABRA1 deletion (Kang et al., 2009). Therefore, it was thought that the patient had absence epilepsy, rather than JME because he lacked the dominant negative effect arising from α1(A322D) subunit. However, our study demonstrates that, at least in mice, Gabra1 deletion is sufficient to cause myoclonic seizures. Possibly, the patient with the 975delC/S326fs328X mutation did not report myoclonic seizures arising during development because they were suppressed from the valproate he had taken since age five (Maljevic et al., 2006) . However, it is also possible other factors such as modifier genes, epigenetic gene regulation, and/or environmental circumstances interact with the heterozygous GABRA1 loss to shape the particular type of genetic generalized epilepsy syndrome epilepsy syndrome experienced by the patient.

$Het_{\alpha1}KO$ and $Het_{\alpha1}AD$ are mouse models of CAE persisting and evolving into JME

A very important result of our study was the finding that the epilepsy phenotype changed during development from P35 to P120. Absence seizures were present in $Het_{\alpha1}KO$ and $Het_{\alpha1}AD$ mice at P35 and persisted until at least P120. Heterozygous Gabra1 deletion and A322D substitution substantially increase the susceptibility to spontaneous and evoked PSDs, and these epileptic abnormalities were significantly more frequent at P120 than P35. In addition, evoked GTC seizures were significantly more frequent at P120 than P35 in all three genotypes of mice, a result showing that brain excitability is increased in mice at that age. Therefore, these mice model the JME subsyndrome, absence epilepsy that persists and evolves into JME (CAE/JME) (Martinez-Juarez et al., 2006;Wirrell et al., 2001;Wirrell et al., 1996).

Importantly, even though age and genotype independently affected seizures, there was no statistically significant interaction between the effects of age and genotype. This result suggests that age confers an independent risk factor for the seizure types found in JME that is additive with the susceptibility conferred by the Gabra1 mutations. Possible mechanisms by which normal brain maturation may increase cerebral excitability and JME-associated seizures have been recently reviewed (Craiu, 2013). Further study of the $Het_{\alpha1}KO$ and $Het_{\alpha1}AD$ mice will help uncover some of these developmental mechanisms.

The CAE/JME subsyndrome accounts for approximately 18% of JME cases and is of particular clinical importance because, unlike classic JME, has a very high rate (93%) of medical intractability (Martinez-Juarez et al., 2006). Although the original description of the GABRA1(A322D) mutation associated it to JME without regard to subsyndrome (Cossette et al., 2002), inspection of the clinical characteristics of patients from the original kindred reveals that two of the eight patients began having seizures at or before age eight, and both of these patients had absence seizures (Cossette et al., 2002). Further analysis suggested that these two patients may have had CAE/JME (Cossette, 2014). It is possible that genetic

modifiers or environmental factors interacted with the two probable human CAE/JME patients to confer the CAE/JME phenotype.

The altered $GABA_AR$ and physiology in M1 layer II/III would be expected to increase seizure susceptibility, but not produce developmental change in phenotype

Compared with wild type, at P35, the frontal cortices in both $Het_{\alpha1}KO$ and $Het_{\alpha1}AD$ mice exhibited similar reductions in α1 subunit expression, similar increases in α3 subunit expression, and no changes in β2/3 or γ2 subunit expression. These results were similar to what was reported previously in P35 $Het_{\alpha1}KO$ mice (Zeller et al., 2008;Zhou et al., 2013). Interestingly, despite the marked changes in total α1 and α3 subunit expression in the cortices of $Het_{\alpha1}KO$ and $Het_{\alpha1}AD$ mice, there was no change in the fraction of total α1 and α3 subunit associated with gephyrin clusters. Therefore, the amount of α1 and α3 subunit at GABAergic synapses directly correlated with total α1 and α3 subunit expression. Cortical $GABA_AR$ receptor expression and physiology (in M1) changed during development with a decrease in α3, β2, and γ2 receptor expression and an increase in mIPSC amplitude. However, these developmentally-associated changes in $GABA_AR$ expression and physiology occurred proportionately in wild type and mutant mice and thus the effects of age and genotype were independent of one another.

Studies of recombinant $GABA_AR$ subunits in cultured cells revealed that, relative to α1βγ receptors, α3βγ receptors had an increased EC_{50} for agonist as well as increased 10-90% rise times and time constants of current decay (Picton & Fisher, 2007;Gingrich et al., 1995). The changes seen here in mIPSC amplitude, rise time, and decay τ in P35 and P120 layer II/III motor cortex are consistent with the increased expression of α3 subunit-containing $GABA_ARs$ and are similar to those seen previously in layer VI pyramidal neurons in the barrel cortex of P35 $Het_{\alpha1}KO$ mice (Zhou et al., 2013). In particular, mIPSC peak current amplitudes were reduced and 10-90% rise times and decay τ were increased. However, our biochemical/immunofluorescence findings do not explain the increase in mIPSC peak amplitudes between P35 and P120 in any of the three genotypes or the difference between $Het_{\alpha1}KO$ and $Het_{\alpha1}AD$ in mIPSC peak amplitude and frequency. This suggests that other factors such as posttranslational modification or vesicular GABA concentration are responsible for these physiological findings.

The effects of heterozygous Gabra1 deletion and A322D substitution on synaptic GABAergic currents would be expected to increase the propensity for seizures. The decreased mIPSC amplitudes seen in both mutant mice could likely contribute to cortical disinhibition. Although the increased mIPSC decay τ and resulting increase in charge transfer could partially compensate for the reduction in mIPSC amplitude in mutant mice, low amplitude, but prolonged inhibition would not be delivered with the same timing as the short, high amplitude inhibition mediated in wild type mice. In addition, it is possible that the increased decay τ could exacerbate seizures because multiple pyramidal neurons innervated by the same GABAergic interneuron would be more tightly synchronized if the GABAergic synaptic currents were prolonged (Mann & Mody, 2008).

The increase in mIPSC amplitude between P35 and P120 would be expected to increase, not decrease, cortical inhibition. Moreover, the effects of age and genotype on amplitude were

statistically independent. Therefore, although changes in cortical synaptic GABAergic inhibition likely contribute the to the formation of seizures at both P35 and P120, developmentally-related changes in GABAergic synaptic inhibition, at least in layers II/III of M1, are not likely to contribute to the worsening of epilepsy phenotype. Further study is needed to determine if age-related changes in $GABA_AR$ expression/function in other brain areas, or non-$GABA_AR$-mediated causes of age-related hyperexcitability (Craiu, 2013) contribute to the developmental expression of myoclonic seizures in $Het_{\alpha 1}KO$ and $Het_{\alpha 1}AD$ mice.

In conclusion, we demonstrated that both $Het_{\alpha 1}KO$ and $Het_{\alpha 1}AD$ mice have similar phenotypes with absence epilepsy that persists and evolves into myoclonic epilepsy and thus they model the human CAE/JME. Both genotypes of mice have altered $GABA_AR$ subunit expression with increased α3 subunit expression at both P35 and P120. The altered $GABA_AR$ composition is associated with reduced synaptic peak currents and altered mIPSC kinetics. Disrupted $GABA_A$-mediated synaptic transmission likely contributes to cortical disinhibition, increased synchrony and seizures, However, other modes of disinhibition, besides changes in $GABA_A$ mediated synaptic transmission in M1, are likely responsible for the worsening of the seizure phenotype from P35 to P120.

Supplementary Material

Refer to Web version on PubMed Central for supplementary material.

ACKNOWLEDGEMENTS

We gratefully acknowledge the support of United States Public Health Service Grant R01 NS064286

REFERENCES

Akman O, Demiralp T, Ates N, Onat FY. Electroencephalographic differences between WAG/Rij and GAERS rat models of absence epilepsy. Epilepsy Res. 2010; 89:185–193. [PubMed: 20092980]

Arain FM, Boyd KL, Gallagher MJ. Decreased viability and absence-like epilepsy in mice lacking or deficient in the $GABA_A$ receptor alpha1 subunit. Epilepsia. 2012; 53:e161–e165. [PubMed: 22812724]

Badawy RA, Vogrin SJ, Lai A, Cook MJ. Patterns of cortical hyperexcitability in adolescent/adult-onset generalized epilepsies. Epilepsia. 2013; 54:871–878. [PubMed: 23551088]

Bartolini E, Pesaresi I, Fabbri S, Cecchi P, Giorgi FS, Sartucci F, et al. Abnormal response to photic stimulation in Juvenile Myoclonic Epilepsy: An EEG-fMRI study. Epilepsia. 2014

Benarroch EE. $GABA_A$ receptor heterogeneity, function, and implications for epilepsy. Neurology. 2007; 68:612–614. [PubMed: 17310035]

Bradley CA, Taghibiglou C, Collingridge GL, Wang YT. mechanisms involved in the reduction of $GABA_A$ receptor alpha 1 subunit expression caused by the epilepsy mutation A322D in the trafficking competent receptor. J Biol Chem. 2008; 283:22043–22050. [PubMed: 18534981]

Camfield CS, Striano P, Camfield PR. Epidemiology of juvenile myoclonic epilepsy. Epilepsy Behav. 2013; 28(Suppl 1):S15–S17. [PubMed: 23756473]

Carvill GL, Weckhuysen S, McMahon JM, Hartmann C, Moller RS, Hjalgrim H, et al. GABRA1 and STXBP1: Novel genetic causes of Dravet syndrome. Neurology. 2014; 82:1245–1253. [PubMed: 24623842]

Cossette P. Personal Communication. 2014

Cossette P, Liu L, Brisebois K, Dong H, Lortie A, Vanasse M, et al. Mutation of GABRA1 in an autosomal dominant form of juvenile myoclonic epilepsy. Nat Genet. 2002; 31:184–189. [PubMed: 11992121]

Craiu D. What is special about the adolescent (JME) brain? Epilepsy Behav. 2013; 28(Suppl 1):S45–S51. [PubMed: 23756479]

Delgado-Escueta AV, Koeleman BP, Bailey JN, Medina MT, Duron RM. The quest for Juvenile Myoclonic Epilepsy genes. Epilepsy Behav. 2013; 28(Suppl 1):S52–S57. [PubMed: 23756480]

Ding L, Feng HJ, Macdonald RL, Botzolakis EJ, Hu N, Gallagher MJ. The $GABA_A$ receptor alpha 1 subunit mutation A322D associated with autosomal dominant juvenile myoclonic epilepsy reduces the expression and alters the composition of wild type GABA-A receptors. J Biol Chem. 2010; 285:26390– 26405. [PubMed: 20551311]

Gallagher MJ, Ding L, Maheshwari A, Macdonald RL. The $GABA_A$ receptor alpha1 subunit epilepsy mutation A322D inhibits transmembrane helix formation and causes proteasomal degradation. Proc Natl Acad Sci U S A. 2007; 104:12999–13004. [PubMed: 17670950]

Garcia-Cabrero AM, Marinas A, Guerrero R, de Cordoba SR, Serratosa JM, Sanchez MP. Laforin and malin deletions in mice produce similar neurologic impairments. J Neuropathol Exp Neurol. 2012; 71:413– 421. [PubMed: 22487859]

Genton P, Thomas P, Kasteleijn-Nolst Trenite DG, Medina MT, Salas-Puig J. Clinical aspects of juvenile myoclonic epilepsy. Epilepsy Behav. 2013; 28(Suppl 1):S8–14. [PubMed: 23756488]

Gingrich KJ, Roberts WA, Kass RS. Dependence of the GABAA receptor gating kinetics on the alpha-subunit isoform: implications for structure-function relations and synaptic transmission. J Physiol. 1995; 489(Pt 2):529–543. [PubMed: 8847645]

Gonzalez MI. The possible role of $GABA_A$ receptors and gephyrin in epileptogenesis. Front Cell Neurosci. 2013; 7:113. [PubMed: 23885234]

Hortnagl H, Tasan RO, Wieselthaler A, Kirchmair E, Sieghart W, Sperk G. Patterns of mRNA and protein expression for 12 $GABA_A$ receptor subunits in the mouse brain. Neuroscience. 2013; 236:345–372. [PubMed: 23337532]

Kang JQ, Shen W, Macdonald RL. Two molecular pathways (NMD and ERAD) contribute to a genetic epilepsy associated with the $GABA_A$ receptor GABRA1 PTC mutation, 975delC, S326fs328X. J Neurosci. 2009; 29:2833–2844. [PubMed: 19261879]

Lachance-Touchette P, Brown P, Meloche C, Kinirons P, Lapointe L, Lacasse H, et al. Novel $\alpha 1$ and $\gamma 2$ $GABA_A$ receptor subunit mutations in families with idiopathic generalized epilepsy. Eur J Neurosci. 2011; 34:237–249. [PubMed: 21714819]

Maljevic S, Krampfl K, Cobilanschi J, Tilgen N, Beyer S, Weber YG, et al. A mutation in the $GABA_A$ receptor alpha(1)-subunit is associated with absence epilepsy. Ann Neurol. 2006; 59:983–987. [PubMed: 16718694]

Mann EO, Mody I. The multifaceted role of inhibition in epilepsy: seizure-genesis through excessive GABAergic inhibition in autosomal dominant nocturnal frontal lobe epilepsy. Curr Opin Neurol. 2008; 21:155–160. [PubMed: 18317273]

Martinez-Juarez IE, Alonso ME, Medina MT, Duron RM, Bailey JN, Lopez-Ruiz M, et al. Juvenile myoclonic epilepsy subsyndromes: family studies and long-term follow-up. Brain. 2006; 129:1269–1280. [PubMed: 16520331]

Picton AJ, Fisher JL. Effect of the alpha subunit subtype on the macroscopic kinetic properties of recombinant $GABA_A$ receptors. Brain Res. 2007; 1165:40–49. [PubMed: 17658489]

Pirker S, Schwarzer C, Wieselthaler A, Sieghart W, Sperk G. $GABA_A$ receptors: immunocytochemical distribution of 13 subunits in the adult rat brain. Neuroscience. 2000; 101:815–850. [PubMed: 11113332]

Reid CA, Kim TH, Berkovic SF, Petrou S. Low blood glucose precipitates spike-and-wave activity in genetically predisposed animals. Epilepsia. 2011; 52:115–120. [PubMed: 21175610]

Robinson PF, Gilmore SA. Spontaneous generalized spike-wave discharges in the electrocorticograms of albino rats. Brain Res. 1980; 201:452–458. [PubMed: 7417856]

Schneider Gasser EM, Duveau V, Prenosil GA, Fritschy JM. Reorganization of GABAergic circuits maintains $GABA_A$ receptor-mediated transmission onto CA1 interneurons in alpha1-subunit-null mice. Eur J Neurosci. 2007; 25:3287–3304. [PubMed: 17552997]

Sitnikova E, van Luijtelaar G. Electroencephalographic characterization of spike-wave discharges in cortex and thalamus in WAG/Rij rats. Epilepsia. 2007; 48:2296–2311. [PubMed: 18196621]

Vollmar C, O'Muircheartaigh J, Symms MR, Barker GJ, Thompson P, Kumari V, et al. Altered microstructural connectivity in juvenile myoclonic epilepsy. Neurology. 2012; 78:1555–1559. [PubMed: 22551729]

Wirrell E, Camfield C, Camfield P, Dooley J. Prognostic significance of failure of the initial antiepileptic drug in children with absence epilepsy. Epilepsia. 2001; 42:760–763. [PubMed: 11422332]

Wirrell EC, Camfield CS, Camfield PR, Gordon KE, Dooley JM. Long-term prognosis of typical childhood absence epilepsy: remission or progression to juvenile myoclonic epilepsy. Neurology. 1996; 47:912–918. [PubMed: 8857718]

Wong M, Wozniak DF, Yamada KA. An animal model of generalized nonconvulsive status epilepticus: immediate characteristics and long-term effects. Exp Neurol. 2003; 183:87–99. [PubMed: 12957492]

Yu ZY, Wang W, Fritschy JM, Witte OW, Redecker C. Changes in neocortical and hippocampal $GABA_A$ receptor subunit distribution during brain maturation and aging. Brain Res. 2006; 1099:73–81. [PubMed: 16781682]

Zeller A, Crestani F, Camenisch I, Iwasato T, Itohara S, Fritschy JM, et al. Cortical glutamatergic neurons mediate the motor sedative action of diazepam. Mol Pharmacol. 2008; 73:282–291. [PubMed: 17965197]

Zhou C, Ding L, Deel ME, Ferrick EA, Emeson RB, Gallagher MJ. Altered intrathalamic GABA neurotransmission in a mouse model of a human genetic absence epilepsy syndrome. Neurobiol Dis. 2015; 73C:407–417. [PubMed: 25447232]

Zhou C, Huang Z, Ding L, Deel ME, Arain FM, Murray CR, et al. Altered cortical $GABA_A$ receptor composition, physiology, and endocytosis in a mouse model of a human genetic absence epilepsy syndrome. J Biol Chem. 2013; 288:21458–21472. [PubMed: 23744069]

HIGHLIGHTS

- Gabra1 knockout and A322D knockin mice have absence seizures at P35 and P120
- Myoclonic seizures are much more frequent at P120 than P35.
- Both mutant mice model absence epilepsy persisting and evolving to JME
- Altered M1 cortex GABAA receptor physiology may explain mutant hyperexcitability
- Changes in M1 $GABA_A$ receptors do not explain evolution of seizure phenotype

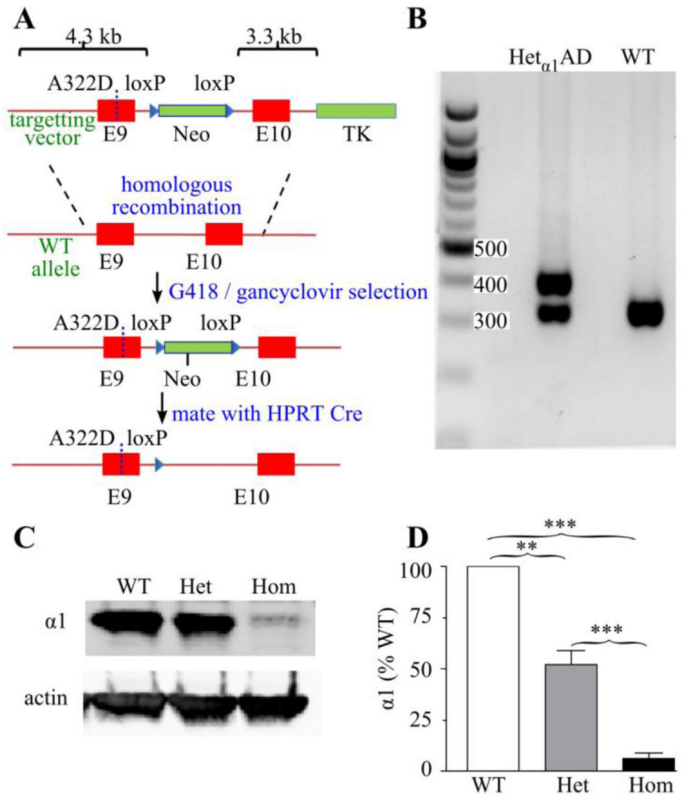

Figure 1. Construction and characterization of Het$_{\alpha1}$AD mice

A) Schematic of the construction of the Het$_{\alpha1}$AD mice. Gabra1 exons are shown in red, selection cassettes (Neo = neomycin, TK = thymidine kinase) are green, and loxP sequences are blue triangles. The BAC targeting vector (top) shows the position of the A322D substitution (dotted line in exon 9). The targeting vector was introduced into the Gabra1 chromosome by homologous recombination and successful incorporations were selected by G418 / ganciclovir treatment. The neomycin cassette was removed by Cre-lox recombination leaving a single loxP sequence. B) Agarose gel of genotyping PCR products showing 324 bp (wild type allele) and 407 bp (mutant allele) products in Het$_{\alpha1}$AD (Het) mice and only 324 bp products in wild type (WT) mice. C-D) Western blots of cortical protein from P15 mice show that compared with wild type mice, Het$_{\alpha1}$AD mice express 52 ± 7% ($P = 0.001$) and Hom$_{\alpha1}$AD mice express 6 ± 3% ($P < 0.001$ vs WT and Het$_{\alpha1}$KO) the amount of α1 subunit protein. ** = $P < 0.01$, *** = $P < 0.001$

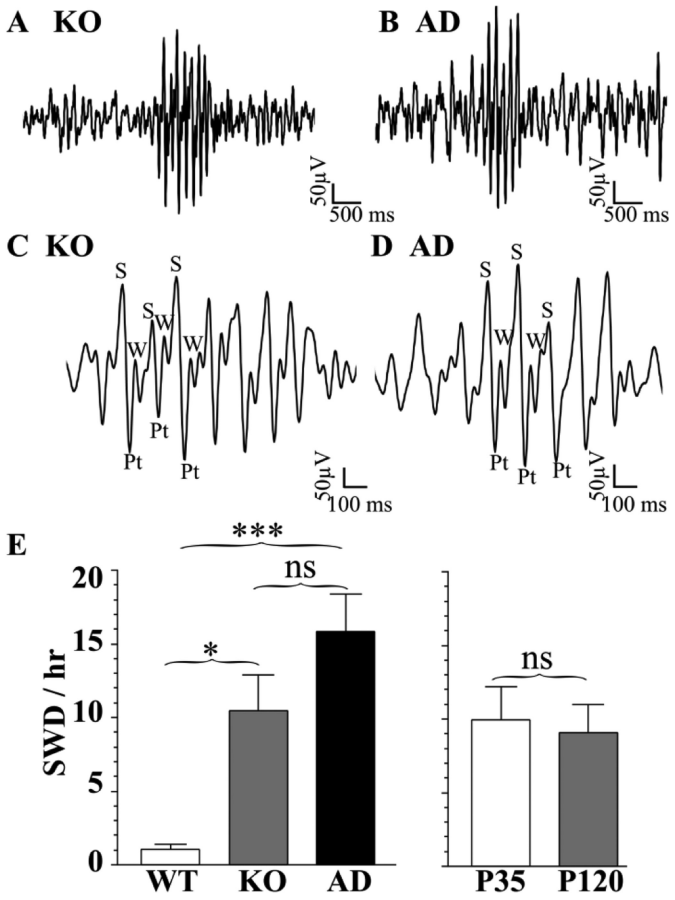

Figure 2. Spontaneous SWDs in $Het_{\alpha 1}KO$ and $Het_{\alpha 1}AD$ mice at P35 and P120

Sample SWDs from $Het_{\alpha 1}KO$ (KO, A, C) and $Het_{\alpha 1}AD$ mice (AD, B, D). When depicted on an expanded time scale (C, D), the SWDs from both mutant genotypes of mice exhibit the typical rodent SWD morphology with rhythmic spikes (S), positive transients (Pt), and waves (W). Two factor ANOVA revealed no interaction between genotype with age on SWD incidence (P = 0.857). However, there was a significant effect of genotype (E) on SWD incidence with a significantly higher SWD incidence in $Het_{\alpha 1}KO$ mice (10.5 ± 2.4 SWD/hr, N = 18, P = 0.012) and $Het_{\alpha 1}AD$ mice (15.8 ± 2.6 SWD/hr, N = 24, P < 0.001) compared with wild type mice (WT, 1.1 ± 0.3 SWD/hr, N = 20). There was no significant difference in SWD incidence between $Het_{\alpha 1}KO$ and $Het_{\alpha 1}AD$ mice (P = 0.189). There was also no effect of age on SWD incidence with 10.0 ± 2.2 SWD/hr, in P35 mice (N = 30) and 9.1 ± 1.9 SWD/hr in P120 mice (P = 0.628, N = 32). ns = nonsignificant, * = P < 0.05, *** = P < 0.001

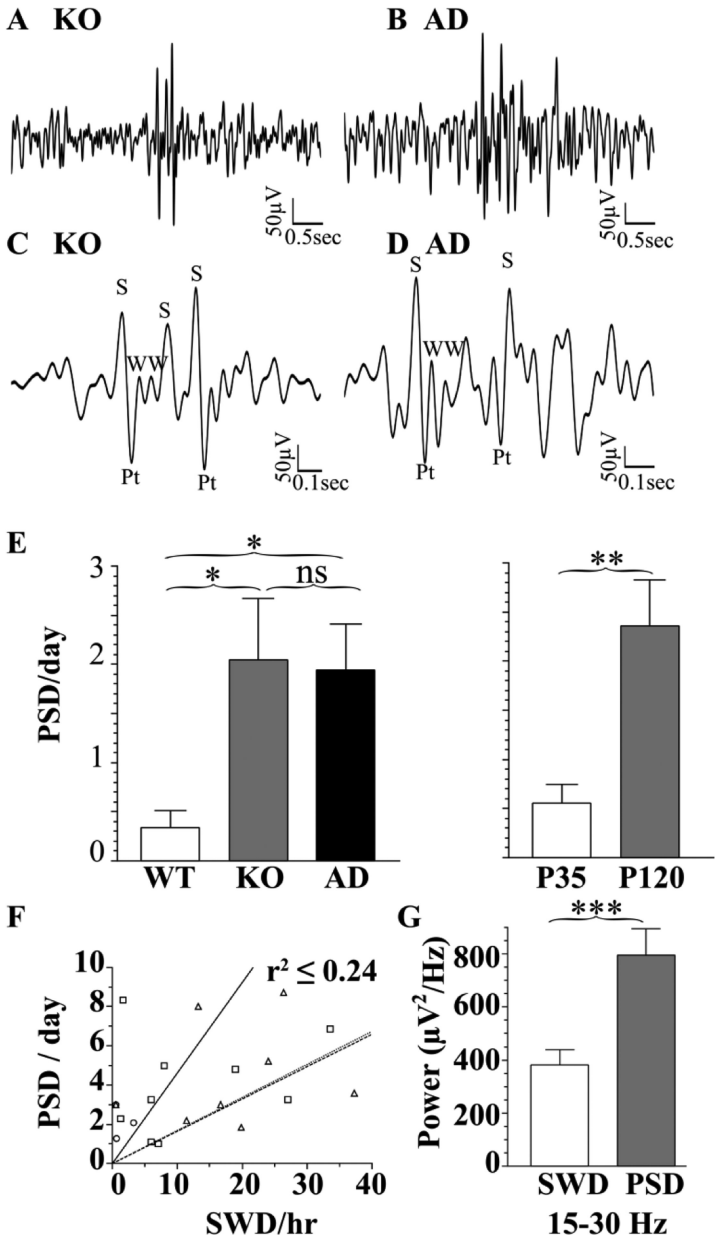

Figure 3. Spontaneous PSDs in $Het_{\alpha 1}KO$ and $Het_{\alpha 1}AD$ mice at P35 and P120

Sample PSDs from $Het_{\alpha 1}KO$ (KO, A, C) and $Het_{\alpha 1}AD$ mice (AD, B, D) show waveforms that differ in morphology and duration from the SWDs (Fig 2). Depiction on an expanded time scale (C, D) reveals that the PSDs are composed of multiple, high frequency, irregular spikes (S) positive transients (Pt), and waves (W). The multiple spikes and waves during the PSDs resulted in an increased high frequency (15-30 Hz) spectral density in PSDs relative to SWDs (G, N = 50 SWDs and N = 49 PSDs). Quantification of PSD incidence (E) shows that, compared with wild type (WT, 0.3 ± 0.2 PSD/day, N = 22), there were more frequent PSDs in $Het_{\alpha 1}KO$ mice (2.1 ± 0.6 PSD/day, P = 0.020, N = 18) and $Het_{\alpha 1}AD$ mice (1.9 ± 0.47 PSD/day, P = 0.016, N = 27). In addition, there were more frequent PSDs at P120 (2.4 ± 0.47 PSD/day, P = 0.001, N =33) than P35 (0.56 ± 0.19 PSD/day, N = 34). There was no

significant difference between $Het_{\alpha 1}KO$ and $Het_{\alpha 1}AD$ PSD incidence and no interaction between genotype and age. For each P120 mouse, the SWD incidence is plotted against the PSD incidence in F; there is no substantial correlation between SWDs and PSDs (WT, circles, solid line, r^2 =0.20, $Het_{\alpha 1}KO$, squares, dashed line, r^2 =0.24, $Het_{\alpha 1}AD$ triangles, dotted line, r^2 = 0.24). ns = nonsignificant , * = $P < 0.05$, ** = $P < 0.01$

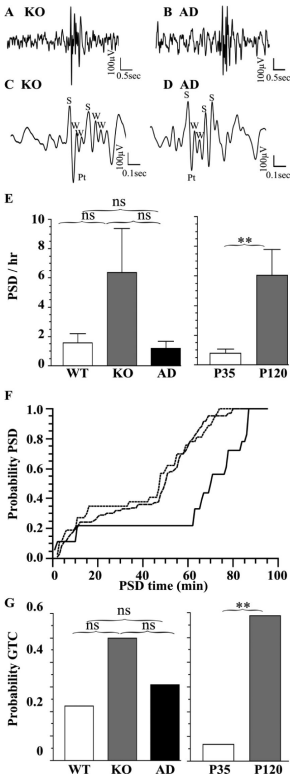

Figure 4. PTZ-evoked PSDs and GTCs in Het$_{\alpha 1}$KO and Het$_{\alpha 1}$AD mice at P35 and P120

PTZ-evoked PSDs from Het$_{\alpha 1}$KO (KO, A, C) and Het$_{\alpha 1}$AD mice (AD, B, D) show a similar morphology to spontaneous PSDs (Fig 3). Depiction on an expanded time scale (C, D) reveals that the PTZ-evoked PSDs are composed of irregular spikes (S) positive transients (Pt), and waves (W). There is no significant difference (E, P ≥ 0.103) in PTZ-evoked PSD among wild type (1.51 ± 0.61 PSD/hr, N = 9), Het$_{\alpha 1}$KO (6.95 ± 3.14 PSD/hr, N = 10), and Het$_{\alpha 1}$AD (2.64 ± 0.79 PSD/hr, N = 13). The P120 mice had a significantly higher PSD frequency (6.3 ± 1.8 PSD/hr, N = 17, P = 0.006) than P35 mice (0.69 ± 0.26 PSD/hr, N = 15). Genotype did alter the PSD latency relative to the time from first PTZ injection (F) with Het$_{\alpha 1}$KO mice (dashed line) and Het$_{\alpha 1}$AD mice (dotted line) having shorter PSD latencies than wild type mice (solid line, P < 0.001). G) The probability of a PTZ-evoked GTC was greater in P120 mice (0.588, P = 0.002) was greater than in P35 mice (0.067), but there was no significant effect of genotype on PTZ-evoked GTCs. ns = nonsignificant, ** = P < 0.01

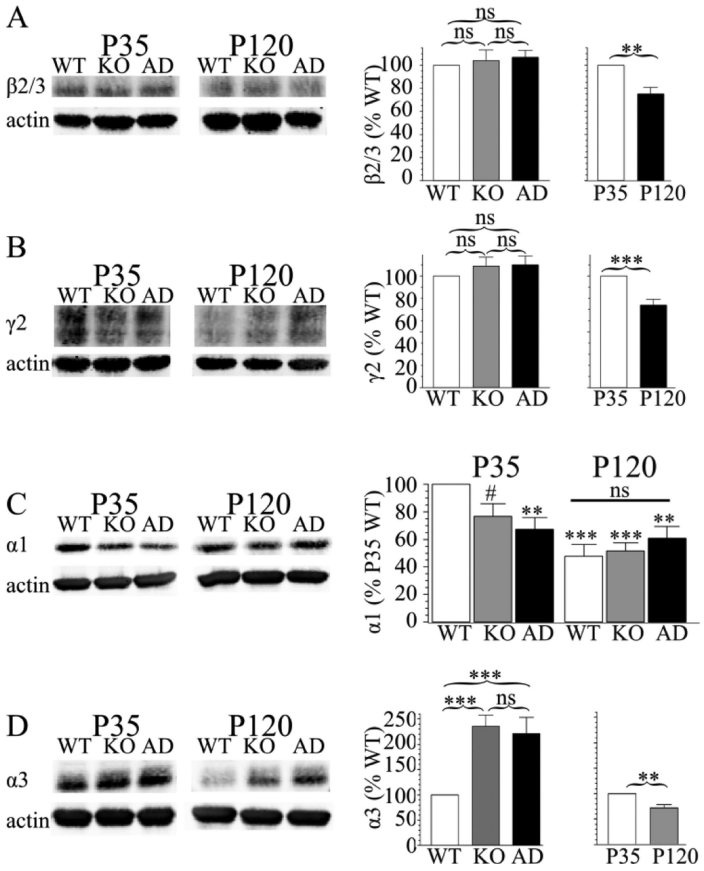

Figure 5. Effects of Gabra1 disruption and development on $GABA_AR$ subunit expression

Western blots of frontal cortex protein depict the effects of age and genotype on $GABA_AR$ subunit protein expression. For each subunit, the P35 and P120 samples are taken from the same gel and are presented with the same brightness and contrast settings; they are shown with a separation because these samples were not run on adjacent lanes of the same gel. Sample size (N) is nine gels for β2/3, γ2, and α3 subunits and eight gels for α1 subunit; all are from three mice of each age and genotype. There was no effect of genotype on β2/3 subunit expression (A, $Het_{\alpha1}KO$ 104 ± 9.4%, $Het_{\alpha1}AD$ 107 ± 6.0%, P ≥ 0.677) or γ2 subunit expression (B, $Het_{\alpha1}KO$ 109 ± 8.0%, $Het_{\alpha1}AD$ 110 ± 7.8%, P ≥ 0.585), but, at P120, there was reduced expression of β2/3 subunit (A, 75 ± 5.9%, P < 0.001) and γ2 subunit (B, 74 ± 5.0%, P < 0.001). There was a significant interaction between age and genotype in α1 subunit expression (C, P = 0.001). At P35, there was reduced α1 subunit expression in $Het_{\alpha1}KO$ (77 ± 9%, #P = 0.077) and $Het_{\alpha1}AD$ (67 ± 8%, P = 0.002), although the reduction in $Het_{\alpha1}KO$ mice was not statistically significant. At P120, wild type cortex had reduced α1 subunit protein expression (48 ± 8%, P < 0.001) than P35 wild type mice. Similarly, compared with P35 wild type mice, there was reduced α1 subunit expression in P120 $Het_{\alpha1}KO$ (56 ± 6%, P < 0.001) and $Het_{\alpha1}AD$ (61± 9%, P = 0.007) cortex. However, at P120, there was no difference in α1 subunit expression among wild type, $Het_{\alpha1}KO$, and $Het_{\alpha1}AD$ cortex (ns, P ≥ 0.463). For α3 subunit expression (D), both $Het_{\alpha1}KO$ (243 ± 42%, P < 0.001) and $Het_{\alpha1}AD$ (223 ± 44%, P < 0.001) had increased α3 subunit expression; there was no difference in α3 subunit expression between $Het_{\alpha1}KO$ and $Het_{\alpha1}AD$ cortex (P =

0.992). There was reduced α3 subunit protein expression at P120 (68 ± 6%, P = 0.002). ns = nonsignificant, ** = P < 0.01, *** = P < 0.001.

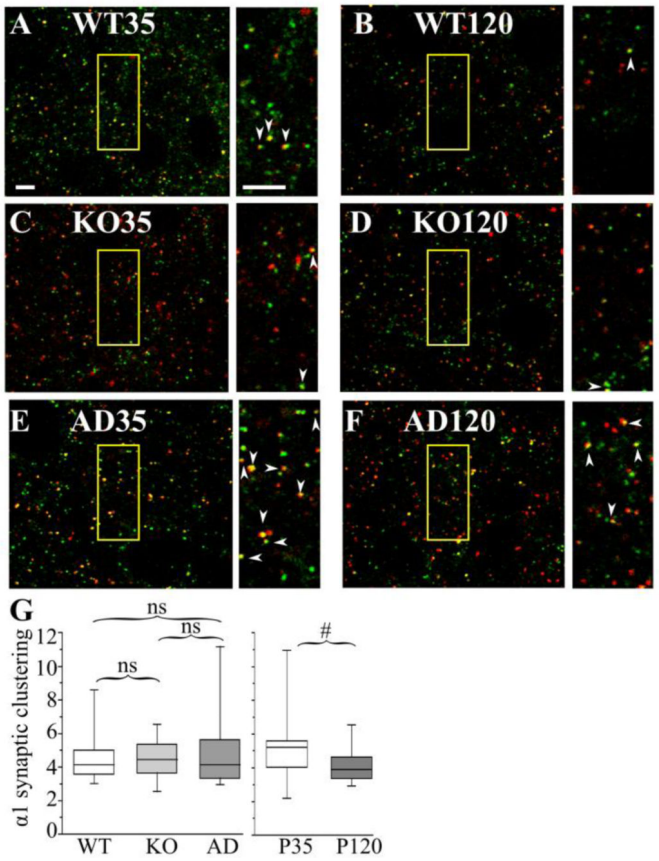

Figure 6. The effects of Gabra1 disruption and age on the association of α1 subunit with gephyrin clusters in layer II/III motor cortex

Confocal microscopic images show P35 (A, C, E) and P120 (B, D, F) wild type (WT, A, B), $Het_{\alpha1}KO$ (KO, C, D), and $Het_{\alpha1}AD$ (AD, E,F) layer II/III motor cortices stained with antibodies directed to α1 subunit (red), and gephyrin (green). The field of view enclosed in the yellow boxes is shown on an expanded scale next to each image. The arrowheads show full or partial overlap (yellow) between gephyrin and the α1 subunit. G) Box plots depict the α1 synaptic cluster ratios with the box length extending from the 25th to 75th percentile and the whiskers extending from the 5th to 95th percentile. The median is marked by the horizontal line. There was no significant difference in synaptic cluster ratio among wild type (median 4.2, 1st-3rd quartile 3.6 – 5.0, N = 14), $Het_{\alpha1}KO$ (median 4.5, 1st-3rd quartile 3.7 – 5.3, N = 14), and $Het_{\alpha1}AD$ (median 4.1, 1st-3rd quartile 3.3 – 5.6, N = 14). The synaptic cluster ratio was reduced at P120 (median 3.9, 1st-3rd quartile 3.4 – 4.7, N = 24) relative to P35 (median 5.2, 1st-3rd quartile 4.0 – 5.6, N = 19), although this difference was not statistically significant (#P = 0.053) Scale bars = 3 μm. ns = nonsignificant.

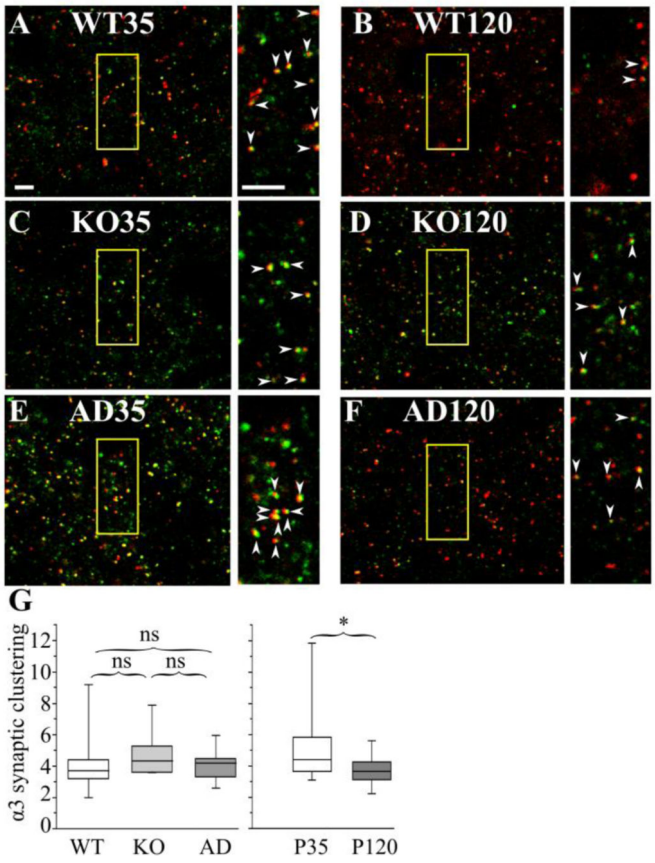

Figure 7. The effects of Gabra1 disruption and age on the association of α3 subunit with gephyrin clusters in layer II/III motor cortex

Confocal microscopic images of P35 (A, C, E) and P120 (B, D, F) wild type (WT, A, B), $Het_{\alpha 1}KO$ (KO, C, D), and $Het_{\alpha 1}AD$ (AD, E, F) layer II/III motor cortices stained with antibodies directed to α3 subunit (red), and gephyrin (green). The field of view enclosed in the yellow boxes is shown on an expanded scale next to each image. The arrowheads show full or partial overlap (yellow) between gephyrin and the α3 subunit. G) Box plots depict the α3 synaptic cluster ratios with the box length extending from the 25^{th} to 75^{th} percentile and the whiskers extending from the 5^{th} to 95^{th} percentile. The median is marked by the horizontal line. There was no significant difference ($P \geq 0.095$) in synaptic cluster ratio among wild type (median 3.7, 1^{st}-3^{rd} quartile: 3.2-4.4, N = 14), $Het_{\alpha 1}KO$ (median 4.4, 1^{st}-3^{rd} quartile: 3.7-5.2, N = 14), or $Het_{\alpha 1}AD$ (median 4.2, 1^{st}-3^{rd} quartile: 3.3-4.5, N = 14). The synaptic cluster ratio was significantly reduced ($P = 0.015$) at P120 (median 3.7, 1^{st}-3^{rd} quartile: 3.1-4.3, N = 24) relative to P35 (median 4.4, 1^{st}-3^{rd} quartile: 3.7-5.8, N = 19), Scale bars = 3 μm. ns = nonsignificant, * = $P < 0.05$.

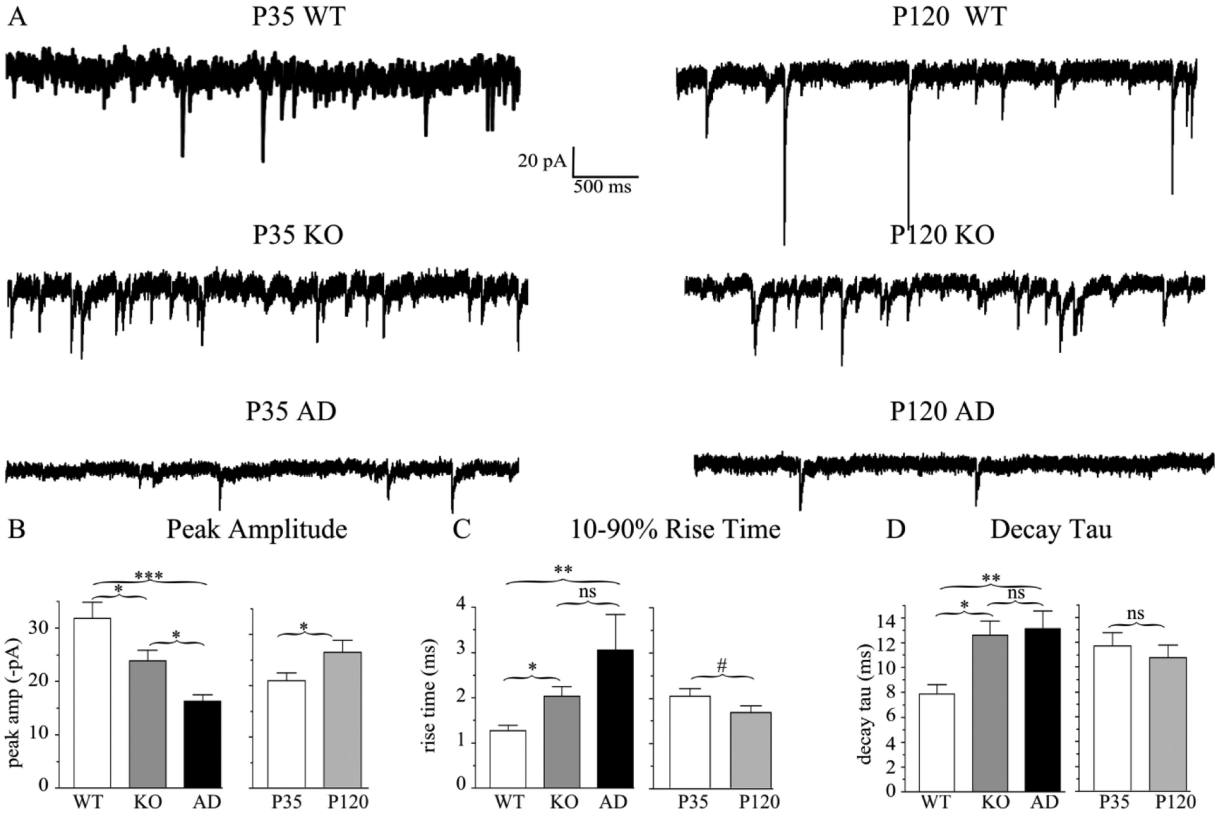

Figure 8. mIPSC peak amplitudes and current kinetic timecourse are altered in Het$_{\alpha 1}$KO and Het$_{\alpha 1}$AD cortex

A) Sample mIPSC traces obtained from P35 (left) and P120 (right) wild type, Het$_{\alpha 1}$KO, and Het$_{\alpha 1}$AD layer II/III pyramidal neurons in the motor cortex. B) Compared to wild type (−31.9 ± 3.0 pA), the magnitude of peak mIPSC amplitude was decreased in Het$_{\alpha 1}$KO (−23.8 ± 2.1pA, P = 0.037) and Het$_{\alpha 1}$AD cortex (−16.3 ± 1.3 pA, P < 0.001). The difference in mIPSC amplitude between Het$_{\alpha 1}$KO and Het$_{\alpha 1}$AD was statistically significant (P = 0.034). The magnitude of mIPSC peak current amplitudes increased from P35 (−21.0 ± 1.6 pA) to P120 (−26.5 ± 2.4 pA, P = 0.030) without any significant interaction between genotype and age. C) The mIPSC 10-90% rise times were greater in Het$_{\alpha 1}$KO (2.0 ± 0.2 ms, P = 0.010 vs. wild type), and Het$_{\alpha 1}$AD (3.1 ± 0.8 ms, P < 0.001 vs. wild type) than wild type neurons (1.3 ± 0.1 ms). The differences in rise times between Het$_{\alpha 1}$KO and Het$_{\alpha 1}$AD neurons (P = 0.677) and P35 (2.0 ± 0.2 ms) and P120 (1.7 ± 0.1 ms, # P = 0.079) mIPSCs were not statistically significant. D) Compared with wild type neurons (7.9 ± 0.8 ms), the decay τ, was increased in Het$_{\alpha 1}$KO (12.6 ± 1.1 ms, P = 0.021) and Het$_{\alpha 1}$AD (13.1 ± 1.4 ms, P = 0.007).There was no significant difference between the values of decay τ at P35 (11.7 ± 1.1 ms) and P120 (10.8 ± 1.0 ms, P = 0.492). Sample sizes (neurons recorded) were N = 18 wild type, 18 Het$_{\alpha 1}$KO, 19 Het$_{\alpha 1}$AD, 26 P35, and 29 P120. * = P < 0.05, ** = P < 0.01, *** = P < 0.001, ns = nonsignificant.

Table 1

Antibodies

Target Protein (conjugation)	Species	Source, Clone/Catalog #	Application(s)	Dilution(s)
Primary antibodies				
actin	Mouse	Developmental Studies Hybridoma Bank, JLA20	WB	1:1000
$GABA_AR$ α1	Mouse	UC Davis/NIH NeuroMab Facility, N95/35	WB	1:250
$GABA_AR$ α1	Rabbit	Millipore, 06868	IF	1:250
$GABA_AR$ α3	Rabbit	Alomone, AGA-003	WB	1:500
$GABA_AR$ α3	Guinea pig	Synaptic Systems 224304	IF	1:500
$GABA_AR$ β2/β3	Mouse	Millipore, 62-3G1	WB	1:300
$GABA_AR$ γ2	Rabbit	Millipore AB5559	WB	1:1000
gephyrin	Mouse	Synaptic Systems, mAb7a	IF	1:100
Secondary antibodies				
guinea pig IgG (Alexa 488)	Donkey	Jackson Immunoresearch, 706-545-148	IF	1:1000
Mouse IgG, (800)	Goat	Licor, 926-32210	WB	1:10,000
Mouse IgM (680)	Goat	Life Technologies, A-21048	WB	1:1000
Mouse IgG, (Alexa 647)	Donkey	Jackson Immunoresearch, 715-605-150	IF	1:500
Rabbit IgG, 680	Goat	Licor, 926-32221	WB	1:10,000
Rabbit IgG, (Cy3)	Donkey	Jackson Immunoresearch, 711-165-152	IF	1:500

WB = Western blot, IF = Immunofluorescence

Table 2

Incidence of spontaneous SWD and PSD and PTZ-evoked PSDs and probability of GTCs

Age	Genotype	Spontaneous SWD/hr ± SE (N)	Spontaneous PSDs/day ± SE (N)	PTZ-evoked PSD/hr ± SE (N)	PTZ-evoked Prob GTC
P35	WT	1.0 ± 0.4 (11)	0.1 ± 0.1 (13)	0.3 ± 0.2 (4)	0.00
	KO	13.0 ± 3.4 (6)	0.2 ± 0.2 (5)	0.2 ± 0.2 (4)	0.00
	AD	16.1 ± 4.0 (13)	1.1 ± 0.4 (16)	1.2 ± 0.5 (7)	0.14
P120	WT	1.1 ± 0.5 (9)	0.7 ± 0.4 (9)	2.5 ± 0.9 (5)	0.40
	KO	9.2 ± 3.3 (12)	2.8 ± 0.8 (13)	11.5 ± 4.4 (6)	0.83
	AD	15.5 ± 3.2 (11)	3.2 ± 0.9 (11)	4.3 ± 1.4 (6)	0.50

WT = wild type, KO = Het$_{\alpha 1}$KO, AD = Het$_{\alpha 1}$AD, PTZ = pentylenetetrazol

Table 3

mIPSC parameters from pyramidal neurons in layer II/III motor cortex

Age	Genotype	# cells	(-) peak amplitude (pA) ± SE	Frequency (Hz) ± SE	10-90% Rise time (ms) ± SE	Decay tau (ms) ± SE	(-) Charge transfer (pA X ms) (1^{st} – 3^{rd} quartile)
P35	WT	8	27.6 ± 2.5	4.9 ± 0.8	1.5 ± 0.2	7.0 ± 1.1	244 (190 - 453)
	KO	9	22.3 ± 2.2	6.8 ± 1.4	2.1 ± 0.3	15.0 ± 1.1	401 (249 - 666)
	AD	9	13.7 ± 0.9	4.6 ± 1.4	2.5 ± 0.3	12.5 ± 2.2	181 (94 - 338)
P120	WT	10	35.3 ± 4.9	4.2 ± 0.4	1.1 ± 0.1	8.6 ± 1.0	446 (436 - 546)
	KO	9	25.4 ± 3.5	6.9 ± 1.8	2.0 ± 0.3	9.9 ± 1.7	468 (403 - 532)
	AD	10	18.6 ± 2.0	1.6 ± 0.5	2.0 ± 0.2	13.7 ± 2.0	251 (172 - 334)

WT = wild type, KO = $Het_{\alpha 1}KO$, AD = $Het_{\alpha 1}AD$